International Journal of Heat and Mass Transfer 196 (2022) 123310

Contents lists available at ScienceDirect

International Journal of Heat and Mass Transfer

journal homepage: www.elsevier.com/locate/hmt

A similarity solution for laminar forced convection heat transfer from solid spheres

Amin M. Elsafi, Mahyar Ashouri, Majid Bahrami*

Laboratory for Alternative Energy Conversion (LAEC), School of Mechatronic Systems Engineering, Simon Fraser University, Surrey, BC, V3T 0A3, Canada

ARTICLE INFO

Article history:
Received 3 June 2022
Revised 24 July 2022
Accepted 27 July 2022

Keywords:
Convective heat transfer
Nusselt number
Sphere
Isoflux
Isothermal
Similarity solution

ABSTRACT

A new analytical solution, based on scale analysis and similarity transformation, is presented to solve a linearized form of the energy equation for the laminar forced convection over a sphere in a spherical coordinate system. Compact expressions for temperature, wall heat flux, and Nusselt number are developed as a function of the Reynolds number (Re_D) and Prandtl number (Pr) for both isothermal and isoflux boundary conditions. A blending method is used to extend the range of the present analytical expression to cover $0 < Re_D < 10^5$ and $0.7 < Pr < \infty$. The present analysis reveals that the theoretical averaged-Nusselt numbers for the laminar forced convection over isoflux (constant wall heat flux) and isothermal (uniform wall temperature) spheres are identical. The proposed model is verified by comparing the analytical expression with the available experimental data over various Reynolds and Prandtl numbers.

1. Introduction

Forced convection heat transfer from a solid sphere is an interesting problem that can be found in many applications. Many experimental studies were conducted to investigate the laminar forced convection heat transfer from an isothermal sphere. Drake and Backer [1] investigated the heat transfer from an isothermally heated sphere to a rarefied gas in a supersonic flow and proposed a correlation for air (Prandtl number, $Pr = 0.7$). Their correlation was applicable for flows with a Reynolds number (Re_D) in the range of $0.1 < Re_D < 2 \times 10^5$. Yuge [2] presented a correlation for the Nusselt number (Nu), for $10 < Re_D < 1.5 \times 10^5$, to estimate the heat transfer from the isothermal spheres to an air flow. Raithby and Eckert [3] conducted a careful study to show the effect of turbulence intensity on the average heat transfer from an isothermal sphere to an air stream within the $3.6 \times 10^3 < Re_D < 5.2 \times 10^4$ range. Whitaker [4] collected and analyzed experimental data from the literature and proposed an easy-to-use correlation for $3.5 < Re_D < 7.6 \times 10^4$ and $0.7 < Pr < 380$. Vliet and Leppert [5] experimentally studied the forced convection heat transfer from an isothermal sphere to liquid water flow. The authors [5] argued that in regions where there was a large temperature difference between the solid surface and water, the effect of the induced natural convection might be significant, and recommended an empirical correlation for calculating the average heat transfer coefficient from isothermal spheres to fluids with $2 < Pr < 380$ for $1 < Re_D < 3 \times 10^4$. Kramers [6] carried out the most comprehensive study for the forced convention heat transfer from a solid sphere using air ($Pr = 0.71$), water ($Pr = 7.3$ and $Pr = 10.7$), and oil ($Pr = 213$ and $Pr = 380$) as fluids to cover a wide range of Prandtl numbers. Will et al. [7] experimentally investigated the forced convection over isothermal spheres with the focus on fluid flows with higher Reynolds numbers ($>3.3 \times 10^5$) than those considered in previous studies. They [7] claimed that there was a critical Reynolds number beyond which there would be a sudden increase in the Nusselt number.

Developing an analytical model to study the forced convection over a sphere is considered a complex task without neglecting the flow separation that occurs at $Re_D > 20$. The analysis of the mass transport process from the surface of a sphere can be used to estimate the heat transfer, i.e., due to the analogy between the two processes. Lee and Barrow [8] used an approximate integral method to solve the integrated boundary-layer equations for axisymmetric flow over a sphere from the forward stagnation up to the point of separation by assuming quartics velocity and temperature profiles. An integral method was also used by Garner and Keey [9] to study the forced convection mass transfer from a sphere at low Reynolds numbers (2.3 to 255). An earlier modeling approach using an integral method was presented by Frössling [10], who estimated the mass transfer rate for a naphthalene droplet evaporating in air ($Pr = 2.53$) by analytically analyzing a laminar boundary layer. Linton and Sutherland [11] compared the heat and mass transfer rates predicted by the theoretical work of Frössling

* Corresponding author.
E-mail addresses: aelsafi@sfu.ca (A.M. Elsafi), mbahrami@sfu.ca (M. Bahrami).

https://doi.org/10.1016/j.ijheatmasstransfer.2022.123310
0017-9310/

Nomenclature

a	radius of a sphere, m
A	surface area of a sphere, m^2
D	diameter of a sphere, m
h	convective heat transfer coefficient, W/m^2-K
k	thermal conductivity, W/m-K
Nu	Nusselt number, -
Pr	Prandtl number, -
r	radial direction, m
Re	Reynolds number, -
T	temperature, K
V	velocity, m/s
$\bar{V}_e$	surface averaged-effective velocity, m/s
$\dot{q}''_w$	wall heat flux, W/m^2

Greek symbols

ρ	density, kg/m^3
β	thermal expansion coefficient, 1/K
α	thermal diffusivity, m^2/s
θ	polar angle, rad
ϑ	non-dimensional temperature, -
η	similarity variable, -
δ_T	thermal boundary layer thickness, m
δ_H	hydrodynamic boundary layer thickness, m
Φ	viscous dissipation, m^2/s^2

Subscripts

∞	related to ambient fluid
w	related to wall

[10] with the experimental data available in the literature for a flow over a sphere. Although, the theoretical local transfer rates were in fair agreement with the experimental data over the front half of the sphere, the results showed that the experimental local values at the front stagnation point were 44% lower than for the theory and differed considerably between studies in the literature.

Several studies were carried out to develop analytical solutions for the forced convection heat transfer from a sphere. Hsu [12] and Sideman [13] derived analytical expressions to estimate the Nusselt number for liquid metals ($Pr \sim 0.01$) flowing past a single sphere by assuming a potential flow. Using the Laplace transform method, Drake and Backer [1] obtained an expression for the Nusselt number by solving a simplified energy equation for the forced convection over an isothermal sphere. Johnstone et al. [14] used a separation of variables method to provide a series solution for the laminar flow over an isothermal sphere by assuming a constant fluid velocity over the sphere. The separation of variables method was also used by Dennis et al. [15], who developed an analytical solution for the forced convection of viscous flows over an isothermal sphere at low values of Reynolds numbers. Ahmed et al. [16] developed an analytical solution for the laminar flow over a sphere by approximating the energy equation to a form of a transient heat conduction equation for which a solution was available. They [16] presented expressions for a surface averaged-effective velocity at two asymptotes ($Pr \ll 1$ and $Pr \gg 1$) and used a blending technique to develop a general expression for the Nusselt number that was valid for $0 \le Re_D \le 2 \times 10^4$ and all Prandtl numbers. The blending method was used earlier by Yovanovich [17] to provide a general expression for the heat transfer coefficient for isopotential spheroids. In another work, Ahmed et al. [18] included the influence of the turbulence level on the heat transfer characteristics in their modeling approach.

Our literature survey suggests that most of the experimental and theoretical studies were focused on forced convection over an isothermal sphere and that there is scarcity of information about isoflux spheres (constant surface heat flux). To the best of our knowledge, there is no study that compared the theoretical heat transfer coefficients for isothermal and isoflux spheres. To this end, the objective of this study is to address this gap by developing new and compact expressions for temperature distribution and heat flux for the laminar forced convection heat transfer from a heated sphere, for both isothermal and isoflux boundary conditions. Both scale analysis and similarity transformation approaches are used to develop new compact models for the isothermal and isoflux cases. The developed models are compared and validated using experimental data available in the literature.

2. Mathematical modeling

2.1. Similarity solution for the energy equation

Fig. 1 schematically shows the temperature profiles in the thermal boundary layer (with a δ_T thickness) for a fluid with an approaching temperature T_∞ and velocity V_∞ flowing over a heated sphere with a radius a (or diameter D). The energy equation is:

$$\rho c_p \frac{\partial T}{\partial t} + \rho c_p \vec{V} \cdot \left(\vec{\nabla} T\right) = \vec{\nabla} \cdot \left(k \vec{\nabla} T\right) + \beta T \frac{Dp}{Dt} + \mu \Phi \tag{1}$$

To simplify the problem, the following assumptions are made:

- Non-porous solid sphere;
- Steady-state heat transfer;
- Incompressible laminar flow ($Re < 10^5$) with constant fluid properties;
- No flow separation;
- Symmetry around the azimuthal angle (2-D problem in r and θ directions);
- Negligible pressure, gravity, and viscous dissipation terms;
- Negligible heat conduction in theθ-direction; and
- Oseen's approximation, i.e., to linearize the convective term (velocity of the fluid around the sphere is everywhere parallel to the surface and is constant) [19]:

$$\left[v_r \frac{\partial T}{\partial r} + \frac{v_\theta}{r} \frac{\partial T}{\partial \theta}\right] \rightarrow \frac{V}{r} \frac{\partial T}{\partial \theta} \tag{2}$$

Accordingly, the energy equation in spherical coordinates reduces to the following:

$$\frac{V}{\alpha} \frac{\partial T}{\partial \theta} = \frac{1}{r} \frac{\partial}{\partial r}\left(r^2 \frac{\partial T}{\partial r}\right) \quad \begin{matrix} r \ge a \\ 0 \le \theta \le \pi \end{matrix} \tag{3}$$

The coordinate system is transformed to set the wall as the coordinate reference. By defining a new coordinate system in the radial direction as $r^* = r - a$, the energy equation becomes:

$$\frac{V}{\alpha} \frac{\partial T}{\partial \theta} = r \frac{\partial^2 T}{\partial r^2} + 2 \frac{\partial T}{\partial r} = r^* \frac{\partial^2 T}{\partial r^{*2}} + a \frac{\partial^2 T}{\partial r^{*2}} + 2 \frac{\partial T}{\partial r^*} \tag{4}$$

By performing a scale (order of magnitude) analysis and considering that $r^* \sim \delta_T$, the terms on the right-hand side of Eq. (4) scale at: $r^* \frac{\partial^2 T}{\partial r^{*2}} \sim \frac{T}{\delta_T}$, $a \frac{\partial^2 T}{\partial r^{*2}} \sim a \frac{T}{\delta_T{}^2}$, and $2 \frac{\partial T}{\partial r^*} \sim 2 \frac{T}{\delta_T}$. One can note that the second term is an order of magnitude larger than the first and third terms. Accordingly, Eq. (4) takes the following simpler form:

$$\frac{V}{\alpha} \frac{\partial T}{\partial \theta} = a \frac{\partial^2 T}{\partial r^{*2}} \quad \begin{matrix} r^* \ge 0 \\ 0 \le \theta \le \pi \end{matrix} \tag{5}$$

By conducting a scale analysis, the scale of the thermal boundary layer thicknessδ_T can be found:

$$\delta_T \sim \sqrt{\frac{\alpha a \theta}{V}} = \frac{\sqrt{2} a \sqrt{\theta}}{\sqrt{Re_D \, Pr}} \tag{6}$$

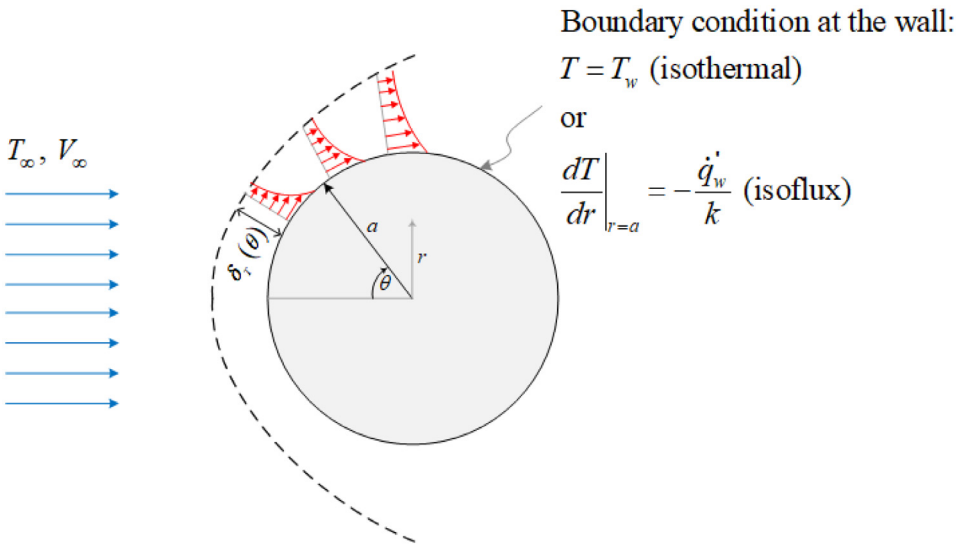

Fig. 1. A schematic diagram of the temperature profiles in the thermal boundary layer.

A non-dimensional similarity parameter η can be defined as:

$$\eta = \frac{r^*}{\delta_T} \tag{7}$$

Eq. 5 is then reduced to an ordinary differential equation that has the following form:

$$\frac{d^2T}{d\eta^2} + \frac{\eta}{2}\frac{dT}{d\eta} = 0 \quad 0 \le \eta \le \infty \tag{8}$$

A non-dimensional temperature can be defined as:

$$\Theta(\eta) = \frac{T(\eta) - T_\infty}{T_w(\eta) - T_\infty} \tag{9}$$

where, T_w is the sphere wall temperature (T_w = const.for isothermal sphere, and $T_w = T_w(\eta)$ for isoflux sphere).

2.2. Isoflux boundary condition

For the case of a sphere with constant heat flux at the wall, the boundary conditions for Eq. (8) are:

$$r = a: \left.\frac{dT}{d\eta}\right|_{r=a} = -a\frac{\dot{q}''_w}{k} \tag{10a}$$

$$r = \infty: T = T_\infty \tag{10b}$$

By solving Eq. (8) after applying the above boundary conditions, the following expression can be used to find the temperature distribution for the isoflux sphere case:

$$T(\eta) = T_\infty + \frac{\sqrt{\pi}}{k}\delta_T \dot{q}''_w\left[1 - erf\left(\frac{\eta}{2}\right)\right] \tag{11}$$

Or, in terms of r and θ :

$$T(r,\theta) = T_\infty + \frac{\sqrt{\pi}}{k}\frac{\sqrt{2}a}{\sqrt{\mathrm{Re}_D\,\mathrm{Pr}}}\dot{q}''_w\left[1 - erf\left(\left(\frac{r-a}{2\sqrt{2}a}\right)\frac{\sqrt{\mathrm{Re}_D\,\mathrm{Pr}}}{\sqrt{\theta}}\right)\right]\sqrt{\theta} \tag{12}$$

The local temperature at the wall, $\eta = 0$, can be determined by:

$$T_w = T_\infty + \frac{\sqrt{\pi}}{k}\delta_T \dot{q}''_w \tag{13}$$

2.3. Isothermal boundary condition

Considering the case in which the wall of the sphere is isothermal, the boundary conditions for Eq. (8) are:

$$r = a: T = T_w \tag{14a}$$

$$r = \infty: T = T_\infty \tag{14b}$$

The temperature distribution for this case in terms of the similarity variable η can be found as:

$$T(\eta) = T_w + (T_w - T_\infty)erf\left(\frac{\eta}{2}\right) \tag{15}$$

The final form of the temperature distribution for the forced convection over an isothermal sphere as a function of r and θ is:

$$T(r,\theta) = T_w - (T_w - T_\infty)erf\left(\left(\frac{r-a}{2\sqrt{2}a}\right)\frac{\sqrt{\mathrm{Re}_D\,\mathrm{Pr}}}{\sqrt{\theta}}\right) \tag{16}$$

The local heat flux temperature at the wall can be evaluated by:

$$\dot{q}''_w = -k\left.\frac{dT}{dr}\right|_{r=a} = -k\left(\left.\frac{dT}{d\eta}\right|_{r=a}\right)\left(\frac{d\eta}{dr}\right) = \frac{1}{\pi}\frac{(T_w - T_\infty)}{\delta_T} \tag{17}$$

3. Results and discussion

Fig. 2(a) and 2(b) show the temperature distribution for flow over a sphere with isoflux and isothermal boundary conditions at the wall, respectively, as evaluated using the expressions developed in this work, Eqs. (12) and (16). For the purpose of showing the temperature variation inside the thermal boundary layer, the results are shown for a low value of Reynolds number ($\mathrm{Re}_D = 1000$) and a Prandtl number on the order of 1. For a sphere with a constant heat flux boundary condition, the wall temperature increases gradually in the angular direction θ and approaches its maximum at $\theta = \pi$ as illustrated by Fig. 2(a).

The temperature profiles at various locations in the thermal boundary layer are shown in Fig. 3(a) and 3(b) for the isoflux and isothermal spheres, respectively.

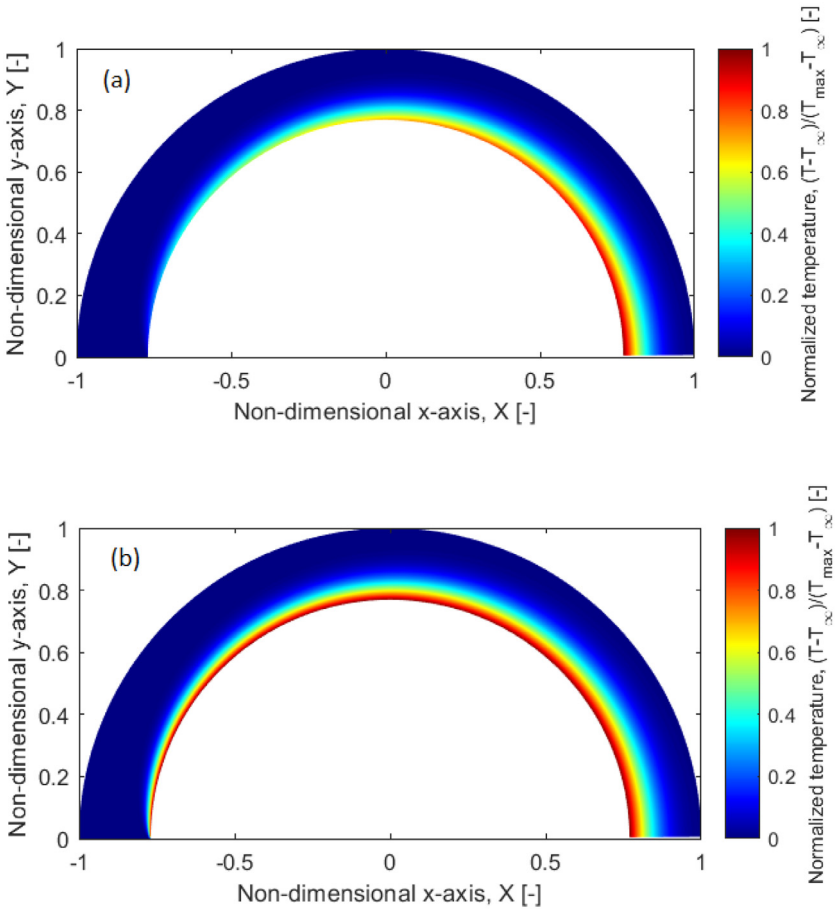

Fig. 2. The temperature distribution for forced convection ($\mathrm{Re}_D = 1000$, $\mathrm{Pr} = 1$) over a sphere with: (a) a constant heat flux of $\dot{q}''_w = 100\mathrm{W/m^2}$; and (b) a uniform wall temperature of $T_w = 80^{\circ}\mathrm{C}$.

3.1. Nusselt number expressions (isoflux and isothermal spheres)

The heat transfer coefficient can be expressed in terms of the Nusselt number, $Nu_D = \frac{hD}{k}$. In the analysis, two heat transfer asymptotes are considered; i) a conduction limit that represents the conduction heat transfer between the body and a surrounding stationary fluid; and ii) the other limit due to the advection (the bulk motion of the fluid) [16,20,21]. Accordingly, the total averaged Nusselt number is determined by:

$$\overline{Nu}_{\text{total}} = \overline{Nu}_{(\text{conduction})} + \overline{Nu}_{(\text{advection})} \tag{18}$$

The conduction limit can by determined by solving the conduction energy equation for a stationary thin fluid film that surrounds a heated sphere, as follows [22]:

$$\frac{\partial}{\partial r}\left(r^2 \frac{\partial T}{\partial r}\right) = 0 \tag{19}$$

For a flow with a constant wall heat flux, the boundary conditions are:

$$r = a: \left.\frac{\partial T}{\partial r}\right|_{r=a} = -\frac{\dot{q}''_w}{k} \tag{20a}$$

$$r = \infty: T = T_\infty \tag{20b}$$

By applying the boundary conditions, the solution for Eq. (19) is:

$$T = \frac{\dot{q}''_w a^2}{k}\frac{1}{r} + T_\infty \tag{21}$$

The temperature at the wall can be evaluated by:

$$T_w = T_\infty + \frac{\dot{q}''_w a}{k} \tag{22}$$

It follows that the conduction limit for an isoflux sphere is:

$$\overline{Nu}_{\text{conduction}} = \frac{\dot{q}''_w (2a)}{k(T_w - T_\infty)} = 2.0 \tag{23}$$

The solution for Eq. (19) for a sphere with an isothermal boundary condition results in the same value ($\overline{Nu}_{\text{conduction}} = 2$).

The Nusselt number, due to the advection, can be obtained by studying the thermal boundary layer. The local value for the Nusselt number along the surface of a sphere is determined by:

$$Nu_{\text{advecion}}(\theta) = \frac{h(2a)}{k} = \frac{\dot{q}''_w (2a)}{k(T_w - T_\infty)} \tag{24}$$

By substitution, the expressions derived using the analysis presented herein for the temperature distribution, Eq. (13), for an isoflux sphere, it follows that:

$$Nu_{\text{advecion}}(\theta) = 0.798\sqrt{\mathrm{Re}_D\,\mathrm{Pr}}(\theta)^{-1/2} \tag{25}$$

Performing the same analysis for the isothermal sphere, Eq. (17) - to find the local heat flux at the wall - results in the same above expression, Eq. (25). Accordingly, the averaged value $\overline{Nu}_D$ can be determined by:

$$\overline{Nu}_D = \frac{1}{A}\iint_A Nu \cdot dA = \frac{1}{2}\int_0^\pi Nu_D \cdot \sin(\theta) d\theta = 0.714\sqrt{\mathrm{Re}_D\,\mathrm{Pr}} \tag{26}$$

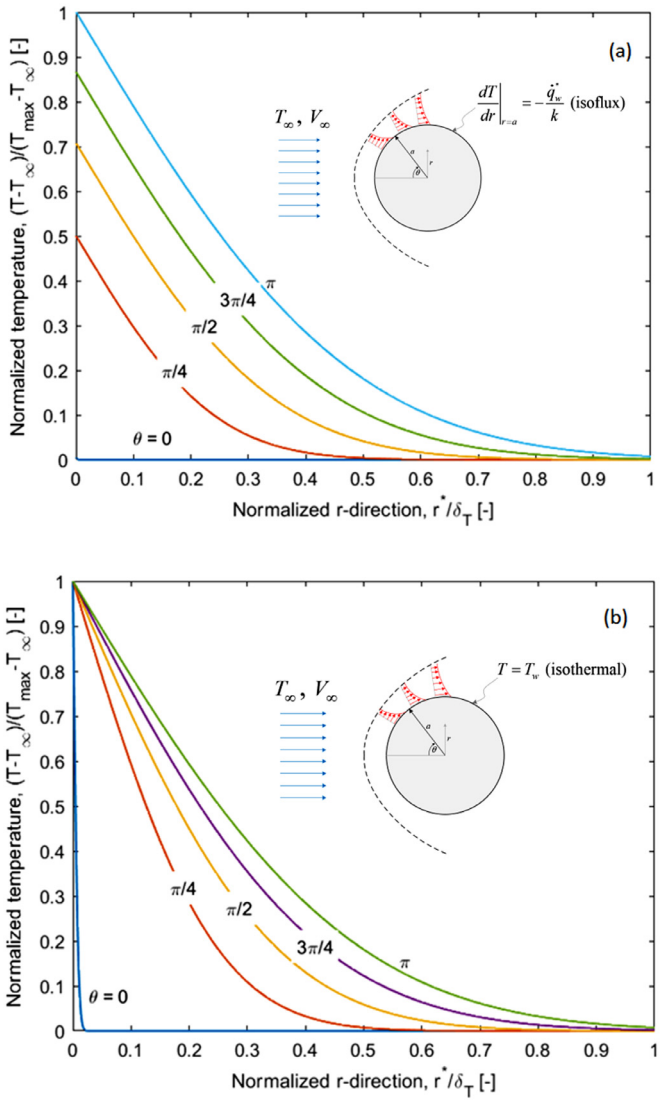

Fig. 3. Normalized temperature profiles at various locations in the thermal boundary layer for: (a) an isoflux; and (b) an isothermal sphere.

Combining Eqs. (18), (23), and (26), the total averaged value for the Nusselt number for the laminar forced convection over a sphere with a uniform wall temperature or constant wall heat flux

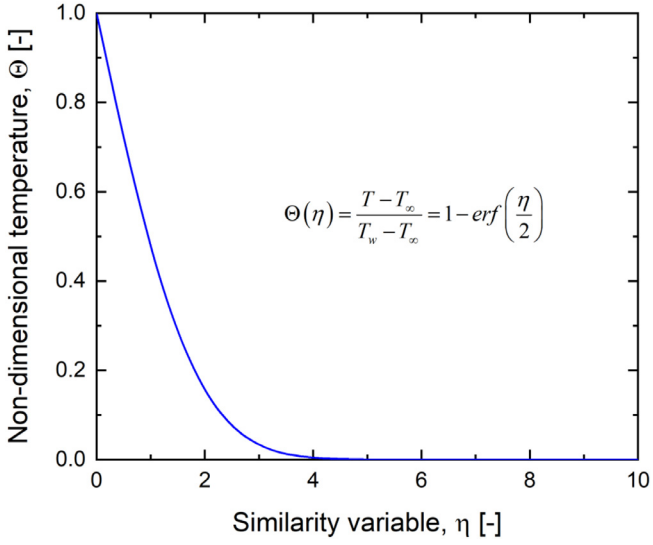

Fig. 5. Non-dimensional temperature distribution,Θ, as a function of the similarity variable η for laminar flow over isothermal and isoflux spheres.

can determined by:

$$\overline{Nu}_D = 2 + 0.714\sqrt{\mathrm{Re}_D\,\mathrm{Pr}} \tag{27}$$

Our analysis indicates that the theoretical Nusselt number for isoflux and isothermal cases are the same, i.e., one expression can be used for both cases. This result can be explained by substituting the expressions for T_w using Eqs. (11) and (15) in Eq. (9) at $\eta = 0$. For both isothermal and isoflux spheres, the non-dimensional temperature distribution, defined by Eq. (9), would be:

$$\Theta(\eta) = 1 - erf\left(\frac{\eta}{2}\right) \tag{28}$$

Interestingly, with this definition, the form of the Nusselt number and the non-dimensional temperature distribution over a sphere with a constant heat flux boundary condition at the wall would be identical to an isothermal sphere as shown in Fig. 4. The non-dimensional temperature profile as a function of the similarity variable η is plotted in Fig. 5. By comparing this figure with Fig. 3(a) and 3(b), it can be observed that all curves collapse onto a single curve. It is worth noting that at $\eta \simeq 5$, there is no change in the temperature gradient, and that the scaling factor for the thermal boundary layer can be considered as 5. Accordingly, the ther-

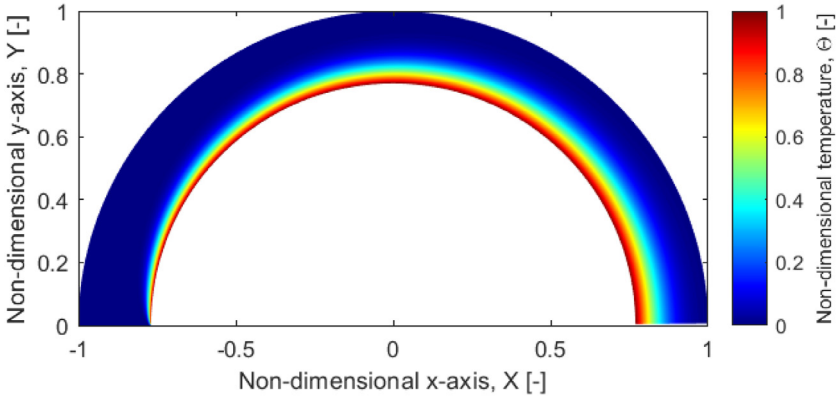

Fig. 4. Non-dimensional temperature distribution (see Eq. (28)) in the thermal boundary layer.

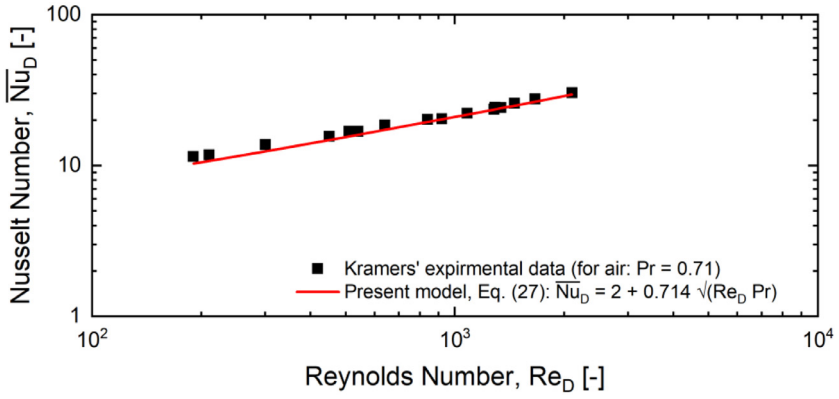

Fig. 6. Validation of Eq. (27) with air experimental data for a sphere with constant wall heat flux (Kramers [6]) .

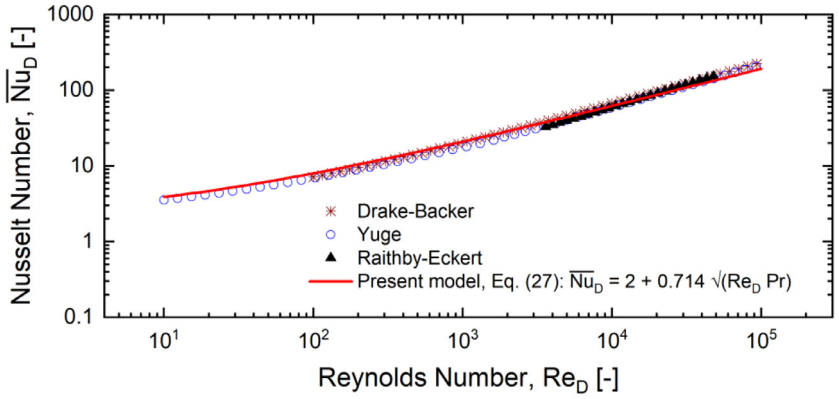

Fig. 7. Validation of Eq. (27) with the empirical correlations developed from the air data for an isothermal sphere (Drake and Backer [1], Yuge [2], and Raithby and Eckert [3]).

mal boundary layer thickness can determine by:

$$\delta_T = 5\sqrt{\frac{\alpha a\theta}{V}} = 5\frac{\sqrt{2}a\sqrt{\theta}}{\sqrt{\mathrm{Re}_D\,\mathrm{Pr}}} \tag{29}$$

3.2. Validation with experimental data

To assess the validity of the presented model for both isoflux and isothermal spheres, the Nusselt number values evaluated using Eq. (27) were compared with the data and empirical correlations available in the literature for both boundary conditions with Pr ~ 1.

The experimental data collected by Kramers [6] (air, Pr = 0.71) for forced convection over sphere is used to validate the isoflux case. In conducting the experiments, Kramers [6] used high frequency heating to induce volumetric heat generation from steel spheres, however; the temperature variation along the wall temperature was not reported. Due to the low thermal conductivity of steel and the low Reynolds numbers at which the experiments were conducted ($\mathrm{Re}_D = 10 - 2000$), the variation in the temperature along the surface of the spheres may be significant and the reported Nusselt number values are actually for a forced convection heat transfer from a sphere with constant heat flux boundary condition at the wall. Fig. 6 shows that Eq. (27) represents a good agreement for Kramers' experimental data.

The empirical correlations developed by Drake and Backer [1], Yuge [2], Raithby and Eckert [3] for a forced convection (of air) over an isothermal sphere were used to assess the validity of Eq. (27) for this case. In these experiments, special care was taken to ensure that there was no variation in the temperature along the surface of the sphere, i.e., the boundary condition at the wall was isothermal. One can observe from Fig. 7 that the Nusselt number values calculated using Eq. (27) are in good agreement with the experimental data for the forced convection over isothermal spheres.

3.3. General expression for Nusselt number

The thickness of the hydrodynamic boundary layer, δ_H, can be greater or less than that of the thermal boundary layer δ_T. The Prandtl number is a non-dimensional number that represents the ratio of the hydrodynamic boundary layer to the thermal boundary layer, and the heat transfer rate is a function of this number, see Eq. (27). The thickness of the hydrodynamic boundary layer is dictated by the velocity profile; therefore, it is important to define the velocity V in Eq. (3). This section is devoted to further verify that the theoretical heat transfer coefficients for both isothermal and isoflux spheres are the same by extending the analysis to cover a wide range of Prandtl numbers. To derive a general expression for the Nusselt number, we use the concept of the area-averaged effective velocity $\overline{V}_e$ discussed by Ahmed et al. [16]. Note that Ahmed et al. [16] transformed the energy equation in the spherical coordinates to a form of a transient heat conduction to derive an expression for the forced flow over an isothermal sphere and the analysis led to the same expression presented here using a similarity solution, Eq. (27). Ahmed et al. [16] assume that velocity is a power-law function of r-direction in order to have a general form for the velocity profiles at different Reynolds number. The use of power–law functions to approximate the velocity profiles throughout the boundary layer was found to be a good assumption as it

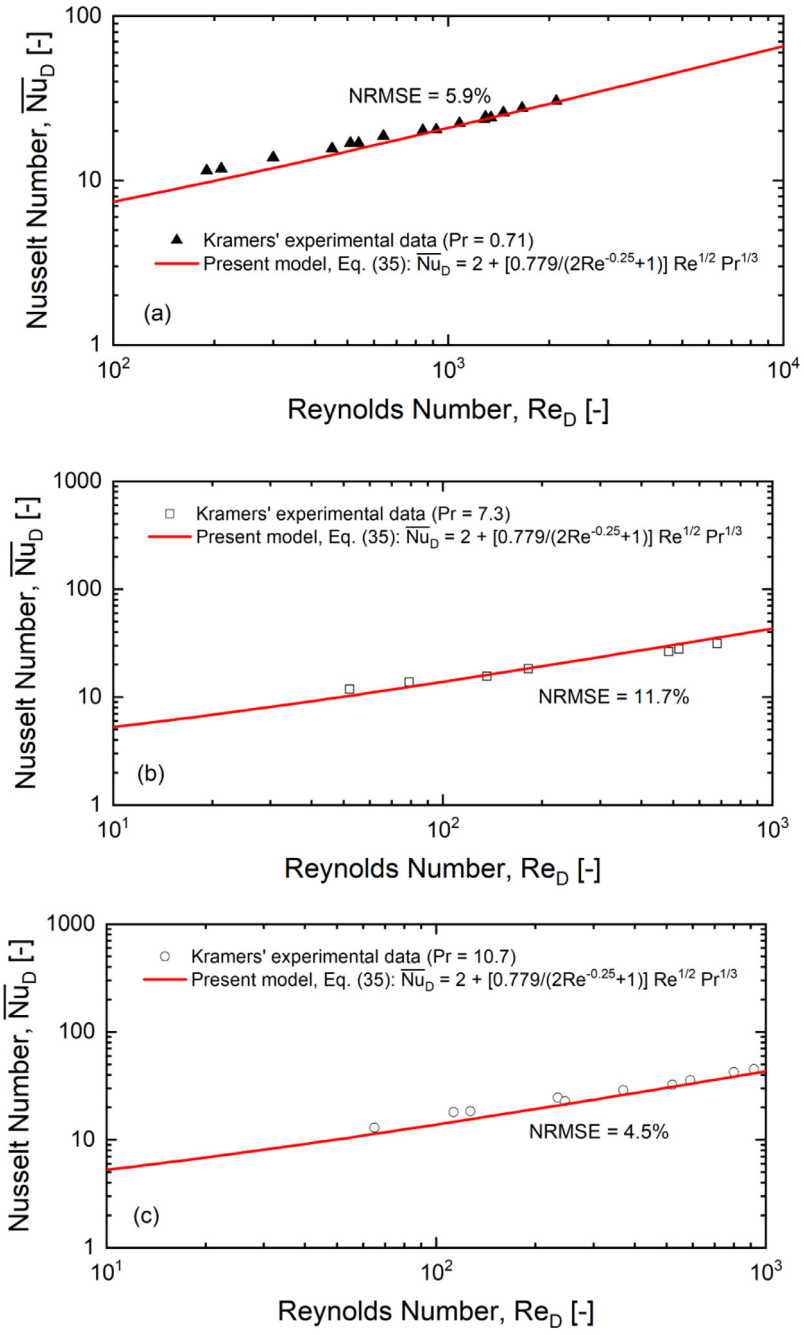

Fig. 8. Validation of the present model, Eq. (35), with the experimental data [6] for an isoflux sphere for: (a) Pr = 0.71, (b) Pr = 7.3, (c) Pr = 10.7, (d) Pr = 213, and (e) Pr = 380.

was used for other geometries [23–25]. Ahmed et al. [16] derived expressions for an area-averaged effective velocity at two asymptotes, namely at $Pr \to 0$ and $Pr \to \infty$:

$$\overline{V}_e^0 = 1.178 V_\infty \text{ when } Pr \to 0 \tag{30}$$

$$\overline{V}_e^\infty = \frac{1.178 V_\infty}{(2\gamma+1)Pr^{1/3}} \text{ when } Pr \to \infty \tag{31}$$

Ahmed et al. [16] used a blending technique to define the area-averaged effective velocity for the entire range of Pr as:

$$\overline{V}_e = \frac{\overline{V}_e^\infty}{\left[1+\left(\frac{\overline{V}_e^\infty}{\overline{V}_e^0}\right)^n\right]^{1/n}} \tag{32}$$

where, n is a fitting parameter determined by comparison against data. By substituting Eq. (20) and (31) into Eq. (32), it follows that:

$$\frac{\left(\overline{V}_e\right)^n}{V} = \frac{1.178/\left[(2\gamma+1)Pr^{1/3}\right]}{\left(1+\left[1/2(2\gamma+1)Pr^{1/3}\right]^n\right)^{1/n}} \quad 0 < Pr < \infty \tag{33}$$

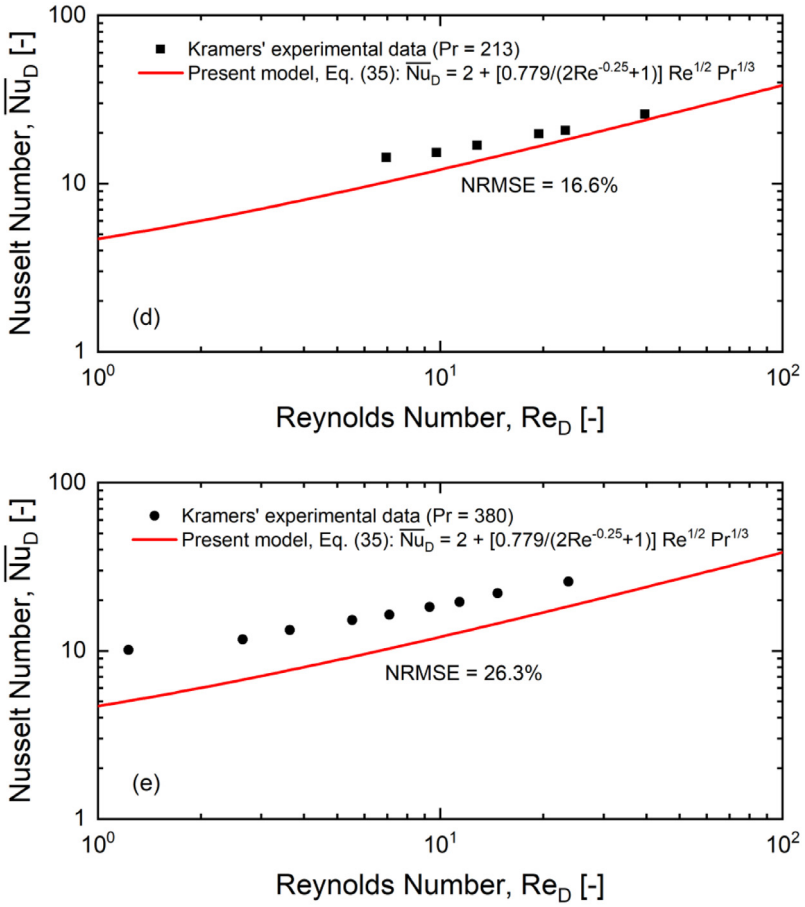

Fig. 8. Continued

In the above equations, the parameter γ defines the form of the velocity profile for various Reynolds numbers. Ahmed et al. [16] suggested $\gamma = 1/\mathrm{Re}^{0.25}$ for a sphere. By substituting Eq. (33) into Eq. (27), a general expression for the Nusselt number can be wirtten as:

$$\overline{Nu}_D = 2 + \frac{0.779}{(2\gamma+1)}\mathrm{Re}_D^{1/2}\frac{\mathrm{Pr}^{1/3}}{\left[1+\left(\frac{1.0}{(2\gamma+1)^3\,\mathrm{Pr}}\right)\right]^{1/2n}} \tag{34}$$

It should be noted that, to find the exponent n that gives the best match for Eq. (34), Ahmed et al. [16] only considered a few correlations for air (Pr = 0.7), namely, Yuge [2], Churchill [26], and Yovanovich [17] correlations, and proposed an exponent of $n = 3$. In the present study, more data and empirical correlations for a wide range of Reynolds and Prandtl numbers were used to find the exponent in the aim to improve the accuracy and range of application of Eq. (34). It includes the data and correlations presented for liquid sodium with Pr = 0.01 (Sideman [13]), air with Pr = 0.7to2 (Drake and Backer [1], Yuge [2], Raithby and Eckert [3], and Clift et al. [27]), water with Pr = 7to10 (Kramers [6], and Vliet-Leppert [5]), and oil with Pr = 213 and Pr = 380 (Kramers [6]). It was found that $n = 500$ gives the best fit for the aforementioned data. It is worth noting that with $n = 500$, the denominator $[1 + (1/(2\gamma+1)^3\,\mathrm{Pr})]^{1/2n}$ in Eq. (34) approaches 1.0. Therefore, the following general expression is proposed for evaluating the Nusselt number for the laminar forced convection over isothermal or isoflux spheres:

$$\overline{Nu}_D = 2 + \frac{0.779}{\left(2/\mathrm{Re}_D^{0.25}+1\right)}\mathrm{Re}_D^{1/2}\mathrm{Pr}^{1/3} \quad \begin{matrix} 0 < \mathrm{Re} < 10^5 \\ 0 < \mathrm{Pr} < \infty \end{matrix} \tag{35}$$

Fig. 8(a) to 8(e) compare the proposed general expression for the Nusselt number with Kramers' experimental data [6] at various Prandtl numbers for an isoflux sphere. The normalized root-mean-square-error (NRMSE, %) is used to estimate the average error between Eq. (35) and the Nusselt number data:

$$NRMSE[\%] = \frac{\sqrt{\sum_{i=1}^{n}\frac{(\hat{y}_i - y_i)^2}{N}}}{\sum_{i=1}^{n}\frac{y_i}{N}} \times 100\% \tag{36}$$

where $\hat{y}_i$ and y_i are the predicted and experimental values, respectively, and N is the number of data points. For air data (Pr = 0.7), the NRMSE is calculated as 5.9%. Considering water data with the Prandtl numbers of Pr = 7.3 and Pr = 10.7, the general analytical expression predicts the Nusselt number values with a NRMSE of 11.7% and 4.5%, respectively. The errors of Eq. (35) from the oil data for Pr = 213 and Pr = 380 are 16.6% and 26.3%, respectively. The low values of NRMSE suggest that Eq. (35) is valid for the forced convention over a sphere with constant flux at the wall as a boundary condition.

Table 1 shows the NRMSE values for the proposed general expression in this work (Eq. (35)) and the Ahmed et al. [16] expression when they are compared with Kramers' data [6]. Both expressions almost have the same error when water and oil data are considered. However, for the air data, Eq. (35) has an error that is 50% lower than the value calculated for the Ahmed et al. expression [16].

Fig. 9(a) to 9(e) are presented to compare the Nusselt number values predicted by Eq. (35) and the Ahmed et al. [16] expression with the correlations presented by Witte [28], Yuge [2],

Table 1
The Normalized root-mean-square-error (NRMSE) values for Eq. (35) and the Ahmed et al. expression.

Fluid	Boundary condition	Reference	Root-mean-square-error, NRMSE [%]	
			Ahmed et al. [16]	Present work, Eq. (35)
Liquid sodium: Pr = 0.01	Isothermal	Witte [28]	83	83.1
Air:	Isoflux	Kramers [6]	11.7	5.9
Pr =	Isothermal	Drake-Backer [1]	23.6	10
0.7	Isothermal	Yuge [2]	14.5	7.9
	Isothermal	Raithby-Eckert [3]	12.4	11.3
Water:	Isoflux	Kramers [6]	11.5	11.7
Pr =	Isothermal	Vliet-Leppert [5]	26.7	24.6
Water: Pr = 10	Isoflux	Kramers [6]	4.4	4.5
Oil: Pr = 213	Isoflux	Kramers [6]	17	16.6
Oil: Pr = 380	Isoflux	Kramers [6]	26.8	26.3

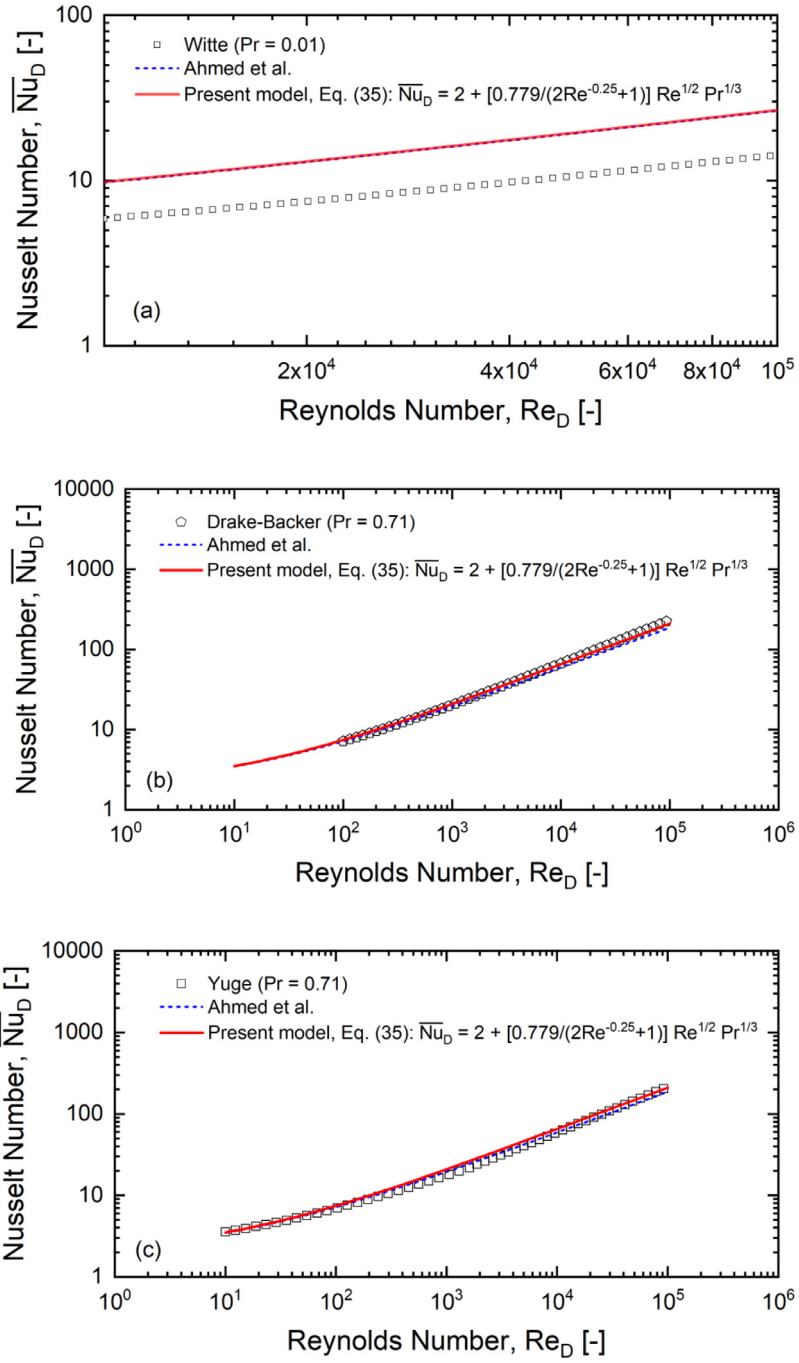

Fig. 9. Validation of the present model, Eq. (35), with the experimental data [1–3,5,28] for an isothermal sphere.

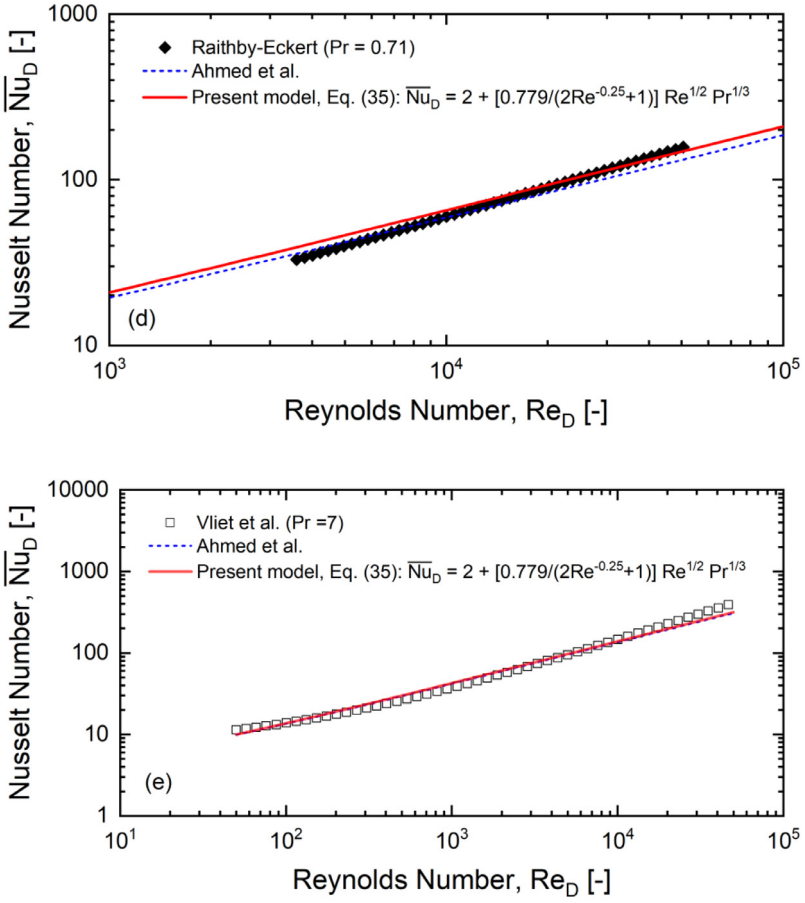

Fig. 9. Continued

Raithby- Eckert [3], Drake-Backer [1], and Vliet-Leppert [5] for the forced convection over an isothermal sphere. The errors of the expressions from the aforementioned correlations are summarized in Table 1. Considering Witte's data [28] for liquid sodium (Pr = 0.01), both expressions tend to overestimate the Nusselt number values (NRMSE=83%), which is probably due to the difference in the velocity profile in Witte's experiments [28] compared to the one assumed in developing the abovementioned expressions. The relatively large errors that result in predicting the Nusselt numbers by using Eq. (35) suggests that perhaps more experimental data at low Prandtl numbers (Pr = 0.01) are needed to develop a better fit. For air data (Pr = 0.7), Eq. (35) has a smaller error than the expression proposed by Ahmed et al. [16]. In some cases, using the Ahmed et al. [16] expression results in errors that are 100% higher than that of Eq. (35) (see NRMSE values for Drake-Backer [1] and Yuge [2] correlations in Table 1). The results presented in Fig. 9(e) and Table 1 show that both expressions have a relatively large error when compared with the correlation proposed by Vliet and Leppert [5] for water data (Pr = 7). Nevertheless, the proposed expression in this work results in an 8% smaller error (NRMSE=24.6%) compared to that calculated for the Ahmed et al. [16] expression (NRMSE=26.7%). These high errors may be attributed to the fact that both expressions do not account for the natural convection in the experiments done by Vliet and Leppert [5] as discussed in the Introduction section. The results presented in Table 1 indicate the validity of Eq. (35) for both isothermal and isoflux spheres and support the conclusion derived earlier about the similarity between the transfer coefficients for the laminar forced convection heat transfer from isoflux and isothermal spheres.

5. Conclusion

The analysis presented in this study revealed that the averaged Nusselt number for the laminar forced convection heat transfer is identical for isothermal and isoflux spheres. This finding was verified by comparing of the proposed model with the experimental data available in the literature. This result may be generalized for packed spheres, and the correlations developed for flow over isothermal spheres can be used to study the heat transfer in packed beds in which heat is generated at the surface of the spheres, as the case with adsorption reactors, without any loss of accuracy. The analytical approach presented herein can be used to derive simple and compact expressions for Nusselt number for other geometries in their respective coordinate systems.

Declaration of Competing Interest

None.

CRediT authorship contribution statement

Amin M. Elsafi: Conceptualization, Methodology, Investigation, Writing – original draft. **Mahyar Ashouri:** Investigation, Writing – review & editing. **Majid Bahrami:** Conceptualization, Supervision, Funding acquisition, Writing – review & editing.

Acknowledgment

The authors gratefully acknowledge the financial support of the Natural Sciences and Engineering Research Council of Canada

(NSERC) through the Advancing Climate Change Science in Canada Grant No. ACCPJ 536076-18.

References

[1] R.M. Drake, G.H. Backer, Heat transfer from spheres to a rarefied gas in supersonic flow, Trans. ASME 74 (1952) 1241–1249.
[2] T. Yuge, Experiments on heat transfer from spheres including combined natural and forced convection, J. Heat Transf. 82 (1960).
[3] G.D. Raithby, E.R.G. Eckert, The effect of turbulence parameters and support position on the heat transfer from spheres, Int. J. Heat Mass Transf. 11 (1968) 1233–1252.
[4] S. Whitaker, Forced convection heat transfer correlations for flow in pipes, past flat plates, single cylinders, single spheres, and for flow in packed beds and tube bundles, AIChE J. 18 (1972) 361–371.
[5] Vliet G.C., Leppert G. Forced convection heat transfer from an isothermal sphere to water 1961.
[6] H. Kramers, Heat transfer from spheres to flowing media, Physica 12 (1946) 61–80.
[7] J.B. Will, N.P. Kruyt, C.H. Venner, An experimental study of forced convective heat transfer from smooth, solid spheres, Int. J. Heat Mass Transf. 109 (2017) 1059–1067.
[8] K. Lee, H. Barrow, Transport processes in flow around a sphere with particular reference to the transfer of mass, Int. J. Heat Mass Transf. 11 (1968) 1013–1026.
[9] F.H. Garner, R.B. Keey, Mass-transfer from single solid spheres—I: transfer at low Reynolds numbers, Chem. Eng. Sci. 9 (1958) 119–129.
[10] N. Frössling, The Evaporation of Falling Drops, Gerlands Beitr. Geophys. 52 (1938) 170–216.
[11] M. Linton, K.L. Sutherland, Transfer from a sphere into a fluid in laminar flow, Chem. Eng. Sci. 12 (1960) 214–229.
[12] C.-J. Hsu, Heat transfer to liquid metals flowing past spheres and elliptical-rod bundles, Int. J. Heat Mass Transf. 8 (1965) 303–315.
[13] S. Sideman, The equivalence of the penetration and potential flow theories, Ind. Eng. Chem. 58 (1966) 54–58.
[14] Johnstone H.F., Pigford R.L., Chapin J.H. Heat transfer to clouds of falling particles. 1941.
[15] S.C.R. Dennis, J.D.A. Walker, J.D. Hudson, Heat transfer from a sphere at low Reynolds numbers, J. Fluid Mech. 60 (1973) 273–283.
[16] Ahmed G.R., Yovanovich M.M. Approximate analytical solution of forced convection heat transfer from isothermal spheres for all Prandtl numbers 1994.
[17] M. Yovanovich, General expression for forced convection heat and mass transfer fromisopotential spheroids, in: 26th Aerosp. Sci. Meet., 1988, p. 743.
[18] G.R. Ahmed, M.M. Yovanovich, J.R. Culham, Experimental and approximate analytical modeling of forced convection from isothermal spheres, J. Thermophys. Heat Transf. 11 (1997) 223–231.
[19] J. Happel, H. Brenner, Low Reynolds number hydrodynamics: with special applications to particulate media. vol. 1, Springer Science \& Business Media, 2012.
[20] Y. Hadad, K. Jafarpur, Laminar forced convection heat transfer from isothermal bodies with unity aspect ratio in coaxial air flow, Heat Transf. Eng. 33 (2012) 245–254.
[21] P.N. Baptista, F.A.R. Oliveira, J.C. Oliveira, S.K. Sastry, Dimensionless analysis of fluid-to-particle heat transfer coefficients, J. Food Eng. 31 (1997) 199–218.
[22] M.N. Ozisik, Heat conduction, John Wiley & Sons, 1993.
[23] I.V. Shevchuk, Turbulent heat and mass transfer over a rotating disk for the Prandtl or Schmidt numbers much larger than unity: an integral method, Heat Mass Transf. 45 (2009) 1313–1321.
[24] I.V. Shevchuk, A new evaluation method for Nusselt numbers in naphthalene sublimation experiments in rotating-disk systems, Heat Mass Transf. 44 (2008) 1409–1415.
[25] I.V. Shevchuk, Modelling of convective heat and mass transfer in rotating flows, Springer, 2016.
[26] S.W. Churchill, A comprehensive correlating equation for laminar, assisting, forced and free convection, AIChE J. 23 (1977) 10–16.
[27] Clift R., Grace J.R., Weber M.E. Bubbles, drops, and particles 2005.
[28] Witte L.C. An experimental study of forced-convection heat transfer from a sphere to liquid sodium 1968.